Optical properties of a suspension of metal spheres

William T. Doyle

Department of Physics and Astronomy, Dartmouth College, Hanover, New Hampshire 03755

(Received 15 August 1988; revised manuscript received 4 January 1989)

The Mie theory is used to find the *in situ* electric dipole polarizability of a sphere of arbitrary size and material. This size-dependent polarizability, together with the Clausius-Mossotti equation, yields an effective dipole generalization of the Maxwell Garnett equation for spheres of nonzero size. Calculated effective optical constants are used to find the reflectance from a suspension of Ag spheres. The results are in good agreement with the recent reflectance measurements of Lee *et al.* [Phys. Rev. B **37**, 2918 (1988)] on porous glass media containing Ag particles.

I. INTRODUCTION

The optical properties of a suspension of small metal particles in a transparent host medium can differ strikingly from those of the same metal in bulk form. Calculation of effective optical constants of such a suspension is extremely difficult, since they intimately involve the wavelength of the radiation, the complex dielectric constant of the metal and the index of refraction of the host medium, the structure, size, and shape of the embedded particles, and the density, orientation, and spatial distribution of the particles. Fortunately, it is often possible to produce suspensions of homogeneous spherical particles with a narrow range of particle size and known spatial distribution. Effective optical constants for the suspension may then be calculated from the known electrodynamic response of a metal sphere.[1]

The effective permittivity may be computed exactly for a regular array of identical spheres. When one or more of the parameters exhibit random variances, however, the problem is less tractable and recourse is usually had to either the Maxwell Garnett or the Bruggemann formula. Although these two formulas agree in the limit of zero particle size and low volume-filling factor, the Maxwell Garnett viewpoint is the appropriate one for this "cermet" topology and is more readily generalized to particles of nonzero size. In this paper we shall use the Mie theory to find an effective dipole generalization of the Maxwell Garnett approach for spherical metal particles of finite size and volume-filling factor. The method is used to calculate the optical properties of monodisperse and log-normal size distributions of small silver particles. Reflectance calculations are compared with the results of recent optical studies of porous glass media containing silver particles.[2]

II. MIE THEORY

A. Exact solution

The orthogonality of the spherical harmonics and the independence of the electric and magnetic partial waves of an isolated sphere permit a separation of the extinction cross section C_{ext} into independent multipole contributions, given by[1,3]

$$C_{\text{ext}} = \frac{2\pi}{k^2} \sum_{n=1}^{\infty} (2n+1)\text{Re}(a_n + b_n) , \tag{1}$$

with

$$a_n = \frac{m\psi_n(mx)\psi_n'(x) - \psi_n(x)\psi_n'(mx)}{m\psi_n(mx)\xi_n'(x) - \xi_n(x)\psi_n'(mx)} \tag{2}$$

and

$$b_n = \frac{\psi_n(mx)\psi_n'(x) - m\psi_n(x)\psi_n'(mx)}{\psi_n(mx)\xi_n'(x) - m\xi_n(x)\psi_n'(mx)} , \tag{3}$$

where ψ_n and ξ_n are the Riccati-Bessel functions. The relative refractive index m is the ratio of the complex index of refraction of the metal n to the real index of refraction n_0 of the host medium. The size parameter x is $2\pi n_0 a /\lambda$, where a is the radius of the particle and λ is the vacuum wavelength.

Although mathematically elegant, the inscrutably concise form of Eqs. (2) and (3) defies physical interpretation. Mie also presented the scattering coefficients a_n and b_n in the alternative form[1,4]

$$a_n = \frac{i(n+1)}{n(2n+1)} \frac{x^{2n+1}}{1^2 3^2 \cdots (2n-2)^2} u_n \frac{m^2 - v_n}{m^2 + [(n+1)/n]w_n} \tag{4}$$

and

$$b_n = \frac{i(n+1)}{n(2n+1)} \frac{x^{2n+1}}{1^2 3^2 \cdots (2n-2)^2} u_n \frac{1 - v_n}{1 + [(n+1)/n]w_n} \tag{5}$$

where each of the functions u_n, v_n, and w_n can be expressed in terms of polynomials and rapidly convergent infinite series in x and mx for which Mie gives explicit expressions. All of the u_n, v_n, and w_n approach unity with vanishing particle radius.

Although Eqs. (2) and (3) are more useful for numerical computations, the alternative forms (4) and (5) exhibit the essential multipole character of the solution, while

displaying the functional dependences of the problem in a physically intuitive way. As a result, they are helpful in providing physical insight and as a guide to physically motivated approximations.

B. Effective polarizability

Equations (1), (4), and (5) show that the electrodynamic response of an isolated sphere of arbitrary size and material in the electric and magnetic fields of a wave of a given wavelength is equivalent to that of a coherent ensemble of ideal *point* multipoles of appropriately chosen size-dependent effective multipole polarizabilities. Each mode is an independent *collective* response driven by the electric and magnetic fields of the corresponding multipole amplitude in the orthogonal expansion of the driving wave.

The effective multipole polarizabilities may be found by dividing each term by the corresponding partial-wave amplitude of the incident wave. For the electric dipole polarizability α_1 we find

$$\alpha_1 = i\frac{3a^3}{2x^3}a_1 \ . \tag{6}$$

This is the exact effective electric dipole polarizability of an isolated sphere. It holds for spheres of any size and material, and it includes the contribution of the host medium. Either of the equivalent expressions (2) or (4) for the scattering coefficient a_1 may be used in Eq. (6).

III. EFFECTIVE MEDIA

A. Effective optical constants

The propagation of an electromagnetic wave in a suspension may be described by an effective index of refraction *for propagation*, even when the particles are not small relative to the wavelength, and effective optical constants, as such, do not exist. The applicability of effective-medium theories to optical problems has been critically examined by Bohren.[5] We need what Bohren calls an *unrestricted* effective-medium theory: one that yields effective optical constants that may be applied in all ordinary optical calculations.

Stroud and Pan[6] used a self-consistent procedure to define an effective permittivity, including the electric and magnetic dipole terms, a_1 and b_1. They applied their result to the problem of the propagation and absorption of far-infrared radiation in metal composites. The magnetic dipole term is needed in their application where eddy-current losses predominate. In our approach the magnetic dipole term could be treated on the same footing as the electric dipole term, by introducing an effective magnetic dipole polarizability. We ignore it here, however, since it makes a negligible contribution relative to the strong electric dipole resonance and it would needlessly complicate the interpretation of optical experiments by necessitating the introduction of an effective magnetic permeability. When still higher multipoles come into play, it is not always possible to describe the general optical behavior of a suspension using effective optical constants.

B. Effective dipole approximation

In seeking a generalization of the Maxwell Garnett equation for spheres of nonzero size, it is helpful to distinguish optically good metals with permittivities having a large Drude free-electron component and small interband absorption from optically poor metals with large interband absorption and a small Drude component. Small spheres of optically poor metals exhibit only a relatively low featureless extinction, while optically good metals exhibit a strong electric dipole resonance. Experiments and calculations based upon the exact Eqs. (1)–(3) typically show that the electric dipole resonance shifts to longer wavelength and broadens, with increasing particle size.[1,3,4] While the interpretation of Eqs. (2) and (3) is obscure, all physical effects accompanying particle growth enter the equivalent Eqs. (4) and (5) via the complex functions u_1, v_1, and w_1. These effects include intensity changes attributable to size-dependent multipole drive efficiencies and skin-depth-induced nonuniform current response. Closer inspection of the functions u_1, v_1, and w_1 in the small-particle limit reveals that the broadening of the extinction peak and the shift toward longer wavelength are produced by the collective nature of the electron motion.[7] All of these physical features are retained by treating the electric dipole term *exactly*, using Eq. (2) for a_1 in Eq. (6).

Equation (4) predicts similar resonances in each of the higher electric multipoles a_n when the real part of the denominator vanishes, but higher multipoles are weighted by increasing powers of the size parameter x and remain small relative to the dominant electric dipole resonance. Moreover, because of the absence of the terms m^2 from Eq. (5), the magnetic multipoles do not exhibit a resonant local-field enhancement. All higher-electric-multipole terms and all magnetic multipole terms will be neglected. Our approximation thus consists in treating the electric dipole term exactly, while setting all other terms a_n and b_n equal to zero. Calculations show that for optically good metals this effective dipole approximation gives excellent agreement with the complete Mie equations in the neighborhood of the dipole resonance.[7] Because the dipole term is treated exactly, this simple approximation exhibits all of the characteristic changes in peak position, intensity, and shape found in the optical experiments. Because it is unencumbered by terms that could hinder its use in effective-medium applications, it is the appropriate generalization of the Maxwell Garnett static polarizability for small particles of optically good metals in the vicinity of the dipole surface-plasmon resonance.

C. Extended Maxwell Garnett theory

The Maxwell Garnett theory involves the dipole approximation in two distinct ways: the individual polarizable entities are treated as dipoles, and only dipole-dipole interactions between the particles are considered. In our approximation, too, a suspension of particles is equivalent to an array of effective point dipoles, so only dipole-dipole interactions can occur. Unless the dipoles are regularly arrayed, even dipole interactions must be

treated approximately. For convenience, and because we want it as a benchmark, we follow the Maxwell Garnett approach and assume that the effective dielectric function of a suspension is related to the dipole polarizability, α_1, by the Clausius-Mossotti equation

$$\frac{K-1}{K+2} = \tfrac{4}{3}\pi N_0 \alpha_1 , \tag{7}$$

where $K = (N/n_0)^2$ is the ratio of the effective permittivity of the suspension to the permittivity of the host, N is the effective index of refraction of the suspension, and n_0 is the real index of refraction of the host medium.

If we insert the effective polarizability from (6) into (9), we have the effective dipole form of the Maxwell Garnett theory for spheres of nonzero size,

$$\frac{K-1}{K+2} = -\frac{2\pi i N_0 a^3 a_1}{x^3} , \tag{8}$$

where the particle number density, N_0, is related in the usual way to the volume-filling factor $f = 4\pi N_0 a^3/3$. The scattering coefficient a_1 is given by either (2) or (4). In the limit of zero particle size, (8) reduces to the Maxwell Garnett equation.

IV. CALCULATED OPTICAL PROPERTIES

A. Particle optical constants

For the permittivity of the metal particles, $\epsilon_m = n^2$, we use the experimental values of Johnson and Christy[8] for the bulk metal permittivity of Ag, ϵ_b, modified to include the additional damping mechanism in the particles introduced by collisions of the conduction electrons with the particle surface.[9] Thus, we set

$$\epsilon_m = \epsilon_b + \frac{\omega_p^2}{\omega(\omega + i/\tau)} - \frac{\omega_p^2}{\omega(\omega + i/\tau + i/\tau_s)} , \tag{9}$$

where ϵ_b, ω_p, and $1/\tau$ are the experimental bulk metal values of the permittivity, plasma frequency, and damping constant, respectively. The quantity $1/\tau_s = u_0/a$ is the surface-collision–damping term, u_0 is the Fermi velocity, and a is the particle radius. In the Maxwell Garnett theory the particle size enters only indirectly through this surface-collision term. This surface-damping term is dominant in very small particles. In larger particles it is overshadowed by the larger explicit size dependences contained in the exact solution.

B. Effective polarizability

Figure 1 shows the real and imaginary parts of the complex effective polarizability of Ag spheres as a function of particle radius. In all of the figures the parameters listed appear in the same order as the peak maxima. The curves for 100-Å-radius particles are almost indistinguishable from the Maxwell Garnett results. For particles smaller than these, there is a progressive broadening of the peaks with decreasing radius and little change in peak position. These size-dependent changes in peak position and width are primarily field-coherence effects.
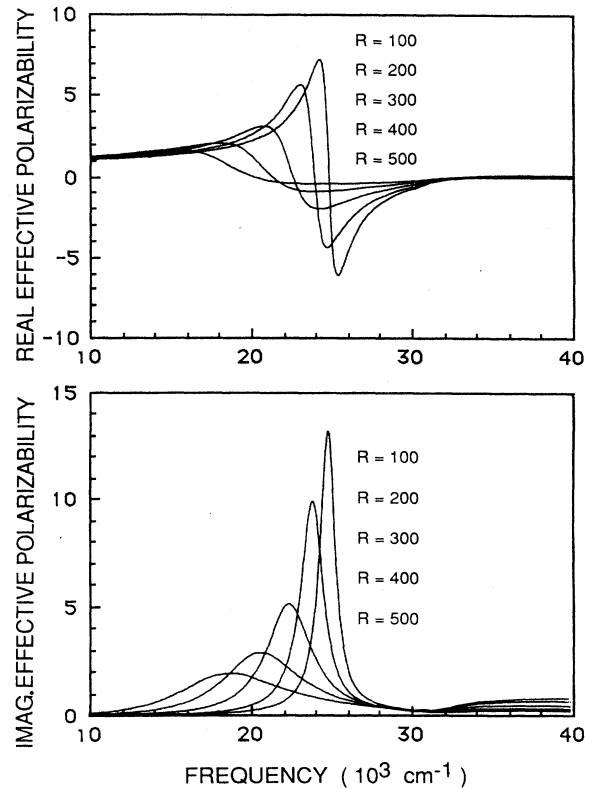

FIG. 1. Calculated frequency dependence of the real and imaginary parts of the complex effective dipole polarizability of Ag particles in porous glass. The host dielectric constant is 2.2 and the particle radius R is in Å. In all of the figures the parameters listed appear in the same order as the peak maxima. The peaks shift to lower frequency with increasing mean radius R and standard deviation σ.

Enhanced radiation damping is the result of collective enhancement of the electric and magnetic fields in the radiation zone of the particle, whereas the peak shift is caused by collective enhancement of the magnetic fields in the near zone of the particle. These purely electrodynamic *collective dipole* effects can be modeled by treating the particle as a giant Thomson atom.[7] They are contained implicity, if obscurely, in the exact Mie solution.

C. Effective optical constants

We can use effective optical constants, $N = N' + iN''$, obtained from the permittivity ratio in Eq. (8), $K = (N/n_0)^2$, in ordinary optical calculations for suspensions, provided the particle densities are large enough to give reliable suspension averages and provided higher-multipole effects can be neglected. Thus the reflectance, R, of a thick sample at normal incidence is given by

$$\mathscr{R} = \left| \frac{(N'-1)^2 + (N'')^2}{(N'+1)^2 + (N'')^2} \right| . \tag{10}$$

D. Reflectance of monodisperse suspensions

Using Eqs. (2) and (8)–(10), we have calculated the reflectance of a suspension of identical Ag spheres for the conditions used in the experiments of Lee et al.:[2] host permittivity $\epsilon_0 = 2.2$ and volume-filling factor $f = 0.036$. Figure 2 shows the calculated reflectance versus frequency for monodisperse spheres for radii ranging from 100 to 500 Å. As expected, on the basis of the effective polarizabilities in Fig. 1, and in qualitative agreement with the experimental results, the reflectance resonance shifts to longer wavelength and broadens with increasing particle size. We should not expect quantitative agreement using a monodisperse size distribution. In contrast with the Maxwell Garnett approximation, the polarizability is now an explicit function of particle radius, and a distribution of particle radii can profoundly influence the calculated optical properties of a suspension. In this approximation the volume-filling factor and average particle radius no longer suffice to determine the optical properties of a suspension. A more complete sample characterization is required.

E. log-normal size distributions

Particles produced by many processes under a wide variety of conditions exhibit size distribution functions that are Gaussian in the logarithm of the particle diameter: the log-normal distribution.[10,11] For spherical particles, the log-normal distribution function, $f_{\text{LN}}(y)$, takes the form

$$f_{\text{LN}}(y) = \frac{1}{(2\pi)^{1/2}\ln\sigma}\exp\left[-\frac{(\ln y - \ln y_g)^2}{2\ln^2\sigma}\right], \quad (11)$$

where y is the particle diameter. The geometrical mean diameter, y_g, and the standard deviation, σ, respectively, are defined by
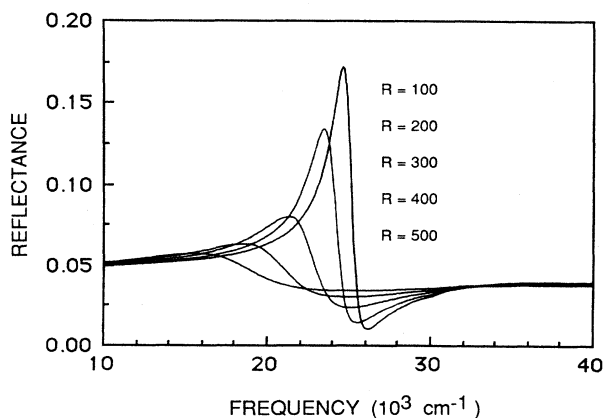

FIG. 2. Calculated frequency dependence of the reflectance of monodisperse suspensions of Ag particles of radius R (in Å) in porous glass media. The host dielectric constant is 2.2 and the volume-filling factor f is 0.036.

$$\ln y_g = \frac{\sum_i n_i \ln y_i}{\sum_i n_i} \quad (12)$$

and

$$\ln\sigma = \left[\frac{\sum_i n_i(\ln y_i - \ln y_g)^2}{\sum_i n_i}\right]^{1/2}, \quad (13)$$

where n_i is the fractional number of particles in the ith equal logarithmic interval $d\ln(y)$ about y_i. In a given suspension the standard deviation in particle size depends on the growth mechanism and on the details of sample preparation. Values of $\sigma = 1.4$–1.6 are commonly encountered.[10]

The log-normal particle-number distribution has the property that all powers of the radius, e.g., the surface and volume distributions, are also distributed log-normally with same standard deviations but with different means.[11] The number average diameter, y_{NL}, is related to the geometric mean diameter, y_g, and the standard deviation, σ, by

$$\ln y_{\text{NL}} = \ln y_g + \tfrac{1}{2}\ln^2\sigma . \quad (14)$$

In our application we are chiefly concerned with volume-weighted distributions, since the quantity of interest, the polarizability, is approximately proportional to the particle volume.

F. Reflectance of heterodisperse suspensions

Reflectance spectra for heterodisperse suspensions were calculated by introducing an assumed mean particle diameter, y_{NL}, and standard deviation, σ, into Eqs. (11) and (14). Then a volume-weighted histogram,

$$f_i = Cy_i^3\frac{dy_i}{y_i}f_{\text{LN}}(y_i), \quad (15)$$

of partial volume-filling factors, $f_i = \tfrac{4}{3}\pi N_{0i}a_i^3$, was constructed and normalized to the total volume-filling factor, f, using the normalization constant C. The factor $dy_i/y_i = d\ln(y_i)$ in (15) is needed with equal diameter-interval sampling cells centered on y_i. In each case the size and number of the sampling cells was chosen to give stable suspension average effective polarizabilities in Eq. (8). The reflectance was calculated using the effective index of refraction, $N = n_0\sqrt{K}$, in Eq. (10).

Figure 3 shows the reflectance spectra at normal incidence of suspensions with log-normal particle-size distributions for a wide range of mean particle radii $R = y_{\text{NL}}/2$ and standard deviations σ. The reflectance curves for $\sigma = 1.0$ correspond to those for the monodisperse distributions shown in Fig. 2. Comparing one panel with another in Fig. 3, we see that all spectra shift toward longer wavelength as the mean particle radius is increased and the standard deviation is held constant. The trend appears clearly in Fig. 2 for $\sigma = 1$. Conversely, the individual panels in Fig. 3 show that the reflectance
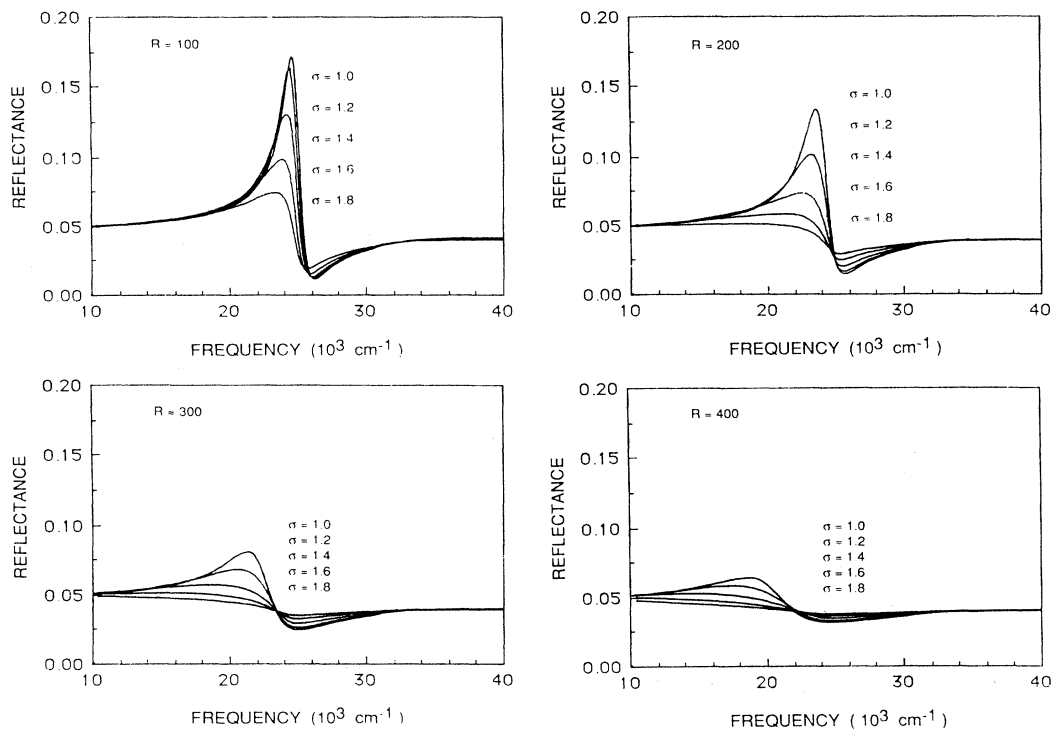
FIG. 3. Calculated frequency dependence of the reflectance of log-normal heterodisperse suspensions of Ag particles in porous glass media. The average radii and the standard deviations of the suspensions are denoted by R (in Å) and σ, respectively.

peaks remain approximately fixed in position, but broaden and decrease in intensity as the standard deviation of the distribution increases and the mean particle radius is held constant.

As the particle distributions widen, the reflection spectra assume a flattened asymmetric shape, much broadened on the low-frequency side and with a sharper characteristic "dip" in reflectance on the high-frequency side of the resonance. This peculiar shape is a consequence of a quadratic dependence of peak position, and a cubic dependence of peak width, on particle radius.[7] Even in very wide distributions the peak position and shape are primarily determined by a smaller range of particles of intermediate size. Contributions from very small particles are suppressed by surface-collision damping, while contributions from very large particles are suppressed by enhanced radiation damping. Since both small and large particles are effectively removed from participation in the peak, the resonance appears severely attenuated in suspensions with a broad size distribution.

V. COMPARISON WITH EXPERIMENT

The recent optical studies of porous glass media containing Ag particles by Lee, Noh, Gaines, Ko, and Kreidler[2] provide a good test of the size dependence predicted by the effective dipole approximation. Silver is an optically good metal and exhibits a sharp dipole resonance. The experimental particle densities studied were large enough to provide reliable suspension averages and the range of particle sizes studied was large enough to cause large changes in the effective optical constants.

In their experiments Lee et al. found a strong size dependence of the reflectance spectrum in the neighborhood of the dipole resonance. They found that the Maxwell Garnett theory gave poor agreement with the position, width, size, and shape of the measured peak in the reflectance spectra. Better agreement with the peak width was obtained using the Persson-Liebsch theory[12] to include random dipole-dipole contributions to the local field. Neither the Maxwell Garnett nor the Persson-Liebsch theory accounted for the peculiar spectral shape observed or for the size-dependent position of the reflectance peak. This is not surprising. Aside from the small effect due to the surface-collision correction to the bulk metal optical constants, there is nothing in either theory that could lead to an explicit size dependence. Moreover, the transmission electron micrographs show that these unique media consist of very-well-separated spherical particles, a distribution consistent with a putative depletion growth mechanism. Such nonrandom distributions would tend to suppress dipole-dipole interaction effects of the type considered in the Persson-Liebsch theory. Random dipole-dipole interactions would be much more difficult to include in a size-dependent theory. Fortunately, they are not needed. The effective dipole approximation, alone, adequately describes the observed reflectance spectra.

OPTICAL PROPERTIES OF A SUSPENSION OF METAL SPHERES

A. Reflectance spectra

Experimental reflectance spectra taken from the measurements of Lee *et al.* are sketched in Fig. 4. The experimental curves for suspensions of spheres with average radii of 110, 270, and 450 Å are shown as dotted-dashed, dashed, and dotted lines, respectively. The peaks shift to lower frequency with increasing mean radius R and standard deviation σ. In order to compare these measured reflectance spectra with the effective dipole theory, it is necessary to consider the width of the particle-size distribution. Although the standard deviations of the experimental distributions are not known, the transmission-electron-microscope pictures for these samples show that they contain well-separated spheres with a wide distribution of particle sizes. Assuming that the distributions are log-normal, we set the average radii, R, equal to the known experimental values and adjust the standard deviations, σ, so that the peak heights roughly match those of the experimental curves. The calculated spectra are shown as solid lines in Fig. 4. The position and width of the reflectance peaks are primarily determined by the experimental average particle radius and are in good agreement with the experimental measurements. The heights of the calculated peaks are primarily determined by the assumed standard deviations. Satisfactory agreement with the peak heights is obtained with values of σ lying within the range commonly observed.

The shape of the reflectance peak is determined by the effective polarizability function, weighted by the assumed particle-size distribution function. For the reasons discussed above, the peak is asymmetric with a pronounced minimum, or "dip," on the high-frequency side of the resonance. Lee *et al.* chose this well-defined spectral feature to characterize the peak position as a function of particle size.
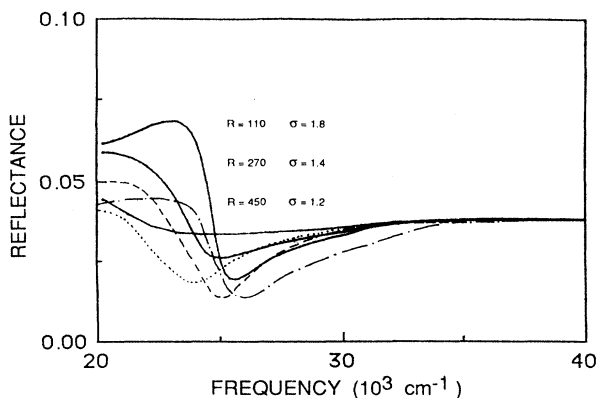

FIG. 4. Comparison of calculated and experimental reflectance spectra for Ag particles in porous glass media. The dotted, dashed, and dotted-dashed lines show the experimental results of Lee *et al.* (see Ref. 2) for suspensions with average particle radii, R, of 450, 270, and 110 Å, respectively. The calculated reflectance spectra are shown as solid lines. In the calculations, the radii, R, were set equal to the experimental values. The (unmeasured) standard deviations, σ, were chosen to match the heights of the experimental peaks.

TABLE I. Summary of reflection-spectra minima.

Mean radius (Å)	Calculated ω_{min} (cm^{-1})	Experimental[a] ω_{min} (cm^{-1})
25	27 100	29 000
70	26 300	26 700
110	26 100	26 000
185	25 600	25 200
270	25 100	25 200
380	24 800	25 000
450	24 800	24 300

[a]See Ref. 2.

While it is easy to measure experimentally, the position of the minimum lacks a simple theoretical significance. It is determined by the combined influence of the position and the width of the resonance, and both are size dependent. The position of the minimum is less sensitive to the standard deviation of the size distribution than to average particle radius. We assume a common standard deviation of 1.0 in Table I, where we compare calculated positions of the minima with the experimental positions.

Given the uncertainty in the experimental particle-size distributions, the agreement between the effective dipole approximation and experiment is good. Since some of the observed particle-size distributions were reported to be bimodal, better agreement might be obtained using histograms of the actual experimental distributions in place of f_{LN} in Eq. (15).

B. Incoherent scattering

With respect to the position, width, intensity, and even the shape of the reflectance peaks, the effective dipole approximation is in satisfactory agreement with experiment. The major discrepancy between the calculated and measured reflectance spectra is an apparent overall depression of the measured reflectance throughout the region of the resonance. The reflectance spectra appear to be superimposed on a smooth background with a broad trough right in the region of the reflectance peak. This discrepancy cannot be removed by adjusting the effective polarizability or filling factor used in the calculations. Decreasing either of these would cause a decrease in peak height on the low-frequency side *and* a shallower dip on the high-frequency side of the reflectance resonance, rather than a depression of both, as observed. For similar reasons, the discrepancy cannot be removed by increasing the standard deviation used in the calculations, or even by introducing a further broadening mechanism, e.g., via random dipole-dipole interactions of the type envisaged by Persson and Liebsch.[12]

In view of the magnitude and length scale of the variances in particle density to be expected under the conditions of the experiments, it is tempting to attribute the apparent overall depression in the measured reflectance to the presence of incoherent scattering from random particle-density fluctuations. This process would remove energy from the specularly reflected beam. Since the incoherent scattering cross section also has a resonance in

the same region of the spectrum as the specular reflection, incoherent scattering from particle-density fluctuations would remove energy from the coherent beam and thus depress the measured specular reflectance throughout the region of the peak, while leaving it almost unchanged at other wavelengths. With a sufficiently detailed knowledge of the particle-density fluctuations one could attempt to correct the calculated specular reflectance for energy losses due to incoherent scattering, but it would be easier and far more reliable to correct the experimental reflectance measurements using measured intensities of the incoherently scattered light. In future experiments it would be helpful to have a detailed characterization of the particle-size distribution, as well as measurements of the non-specular-scattered light intensity as a function of wavelength and angle.

VI. CONCLUSION

The electrodynamic response of an isolated sphere is equivalent to that of a coherent ensemble of ideal point multipoles with appropriately chosen size-dependent multipole polarizabilities. The effective multipole polarizabilities can be obtained by dividing the Mie-scattering coefficients by the corresponding partial-wave amplitudes of the incident wave. These polarizabilities hold for spheres of arbitrary size and material and include the effect of a host medium. For small particles of optically good metals, such as silver, the electric dipole term alone gives a good approximation to the exact solution in the neighborhood of the strong dipole resonance.

Combining the effective dipole polarizability with the Clausius-Mossotti equation yields a size-dependent generalization of the Maxwell Garnett theory for the effective material constants of a suspension. In the absence of higher multipole contributions, the effective optical constants may be used in conventional optical calculations. In this approximation the distribution in particle size must be taken into account. The method can be used with experimental size distributions, when these are available. Assuming a log-normal size distribution, calculated reflectances are in good agreement with the size dependence of the position, width, and shape of the resonant peaks observed in recent reflectance measurements on porous glass media containing silver particles.

[1]G. Mie, Ann. Phys. (Leipzig) **25**, 377 (1908).

[2]S.-I. Lee, T. W. Noh, J. R. Gaines, Y.-H. Ko, and E. R. Kreidler, Phys. Rev. B **37**, 2918 (1988).

[3]C. F. Bohren and D. R. Huffman, *Absorption and Scattering of Light by Small Particles* (Wiley, New York, 1983), p. 101.

[4]M. Kerker, *The Scattering of Light and Other Electromagnetic Radiation* (Academic, New York, 1969), p. 83.

[5]C. F. Bohren, J. Atmos. Sci. **43**, 468 (1986).

[6]D. Stroud and F. B. Pan, Phys. Rev. B **17**, 1602 (1978).

[7]W. T. Doyle, J. Opt. Sci. Am. A **2**, 1031 (1985).

[8]P. B. Johnson and R. W. Christy, Phys. Rev. B **6**, 4370 (1972).

[9]W. T. Doyle and A. Agarwal, J. Opt. Soc. Am. **55**, 305 (1965).

[10]C. F. Granquist and R. A. Buhrman, J. Appl. Phys. **47**, 2200 (1976).

[11]T. Allen, *Particle Size Measurement* (Wiley, New York, 1968), p. 95.

[12]B. N. J. Persson and A. Liebsch, Solid State Commun. **44**, 1637 (1982); A. Liebsch and B. N. J. Persson, J. Phys. C **16**, 5375 (1983); A. Liebsch and P. V. Gonzalez, Phys. Rev. B **29**, 6907 (1984).